Available online at www.sciencedirect.com
ScienceDirect
Acta Materialia 55 (2007) 3749–3756
Acta MATERIALIA
www.elsevier.com/locate/actamat

What is behind the inverse Hall–Petch effect in nanocrystalline materials?

C.E. Carlton, P.J. Ferreira *

Materials Science and Engineering Program, University of Texas at Austin, Austin, TX 78712, USA

Received 11 January 2007; accepted 18 February 2007
Available online 8 April 2007

Abstract

An inverse Hall–Petch effect has been observed for nanocrystalline materials by a large number of researchers. This effect implies that nanocrystalline materials get softer as grain size is reduced below a critical value. Postulated explanations for this behavior include dislocation-based models, diffusion-based models, grain-boundary-shearing models and two-phase-based models. In this paper, we report an explanation for the inverse Hall–Petch effect based on the statistical absorption of dislocations by grain boundaries, showing that the yield strength is dependent on strain rate and temperature and deviates from the Hall–Petch relationship below a critical grain size.

Keywords: Nanocrystalline materials; Dislocations; Grain boundaries; Theory; Plastic deformation

1. Introduction

Nanocrystalline materials show promise for applications in a wide range of fields, particularly because of their high strength-to-weight ratios when compared with their coarse-grained counterparts. However, the high strength expected for nanocrystalline materials has been questioned by several investigations, which claimed a decrease in the yield stress σ_y below a critical grain size [1–11]. A great deal of effort has been expended studying and attempting to explain this effect, but controversy still persists [12–34]. However, as evidence of this unique behavior emerges, a crucial question arises: As the structural scale reduces from the micro to the nanometer range, how does the yield stress change with grain size and what are the operating mechanisms?

Classically, one would expect an increase in σ_y for smaller grain sizes according to the Hall–Petch equation [35,36] given by

$$\sigma_y = \sigma_0 + kd^{-1/2} \tag{1}$$

where σ_0 is the friction stress in the absence of grain boundaries, k is a constant and d is the grain size. In other words, the yield stress increases as grain size decreases because pile-ups in fine-grained materials contain fewer dislocations, the stress at the tip of the pile-up decreases and, thus, a larger applied stress is required to generate dislocations in the adjacent grain. In very small grains, this mechanism will break down because grains are unable to support dislocation pile-ups. Typically, this is expected to occur for grain sizes below 10 nm for most metals [12,37]. As a consequence, a threshold value is expected at which a maximum yield stress can be achieved. However, experimentally, several systems such as Cu and Ni have revealed that the Hall–Petch slope (k value in Eq. (1)) is reduced or becomes negative below a certain grain size [1,2,4–10]. This is known as the inverse Hall–Petch effect (IHPE). Furthermore, the transition in the Hall–Petch slope normally occurs for grain sizes above 10 nm, where dislocation pile-ups are still possible.

So far, most of the models proposed to explain the IHPE behavior fall into at least one of four categories,

* Corresponding author. Tel.: +1 512 471 3244; fax: +1 512 471 7681.
E-mail address: ferreira@mail.utexas.edu (P.J. Ferreira).

1359-6454/$30.00
doi:10.1016/j.actamat.2007.02.021

namely dislocation-based models [13–17], diffusion-based models [18,19], grain-boundary-shearing models [20–23] and two-phase-based models [24–29].

The dislocation-based models assume that dislocation motion is the primary agent for plastic flow in nanocrystalline materials and explain the IHPE by taking into account the ways that very small crystallite sizes can affect the behavior of dislocations. For example, one model considers how the energy of a dislocation may be reduced by a very small crystal and how the change in the dislocation's energy could affect its motion and lead to the IHPE [13]. Another dislocation-based model considers how a nanocrystalline grain could affect the operation of Frank–Reed dislocation sources [14]. Additionally, molecular dynamics simulations of some metals indicate that deformation of nanocrystalline materials can occur via a dislocation mechanism [16].

The diffusion-based models assume various diffusion processes to explain the IHPE. In one model, the IHPE is attributed to the effect of Coble creep in strain rate regimes and temperature ranges where it is not normally seen [18]. Some models use diffusion processes in combination with other mechanisms to explain the IHPE. For example, one model explains the IHPE using a combination of dislocation motion and creep [15], while another model explains the IHPE as being due to grain-boundary shear by a thermally activated grain-boundary-shearing mechanism [19].

A third set of models suggest that grain-boundary shearing is the dominant cause for the IHPE behavior. Grain-boundary shearing has been observed in various molecular dynamics simulations [20,22,23]. In these simulations, grain-boundary shearing begins to dominate dislocation motion as the primary means of deformation at very low grain sizes. There are also analytical models that use grain-boundary shearing to explain the IHPE. In one of these models, grain boundaries and crystalline grains are considered to be separate phases, much like the two-phase models mentioned below. In this model the grain boundary is assumed to deform by an athermal grain-boundary-shear mechanism while the grain interior behaves normally [21].

Finally, another set of models explain the IHPE by considering a nanocrystalline material to be a composite material with at least two phases, namely a grain-boundary phase and a grain-interior phase [23–28]. In one of these models, the grain boundary is considered a continuous material that is strengthened by nanocrystalline grains in much the same way that conventional materials can be strengthened by precipitates [27]. In another model, the grain-boundary material and the lattice material are assumed to have different yield strengths [26]. A third model assumes quite special mechanical properties for the grain boundary [28].

Considering the aforementioned volume and good quality of the work completed on explaining the IHPE in metals, it is necessary to justify the publication of a new model. This motivation arises because recent experimental evidence related with the IHPE has indicated that many of the proposed models may be inadequate for explaining the IHPE. Among of the most important experimental findings in this regard are several in situ transmission electron microscopy (TEM) observations of dislocation motion during tensile deformation and nanoindentation of nanocrystalline materials [38–45]. This is relevant because many of the models listed above are based on the assumption that dislocation motion does not play a significant role in the deformation of nanocrystalline materials. In addition, many of the same TEM studies have also shown that plastically deformed nanocrystalline materials contain a very low accumulated dislocation density. These observations are contrary to models that rely on strain hardening as the means to understand the Hall–Petch relationship [13,15].

Finally, a recent experiment, where the strain rate sensitivity of nanocrystalline copper was determined by nanoindentation, revealed that nanocrystalline materials should be more strain-rate sensitive than their microcrystalline counterparts, but not as sensitive as Coble creep models would suggest [46].

In the context of this lively and continuing discussion, the purpose of this paper is thus to suggest a model for the IHPE in nanocrystalline materials based on the nature of dislocation absorption by grain boundaries. The paper will show that below a critical grain size, typically at the nanoscale, dislocations are more easily absorbed by grain boundaries. The model matches in situ TEM observations, which show that dislocations remain relatively active in nanocrystalline materials [38–45], while the dislocation density remains considerably low.

2. A model for the inverse Hall–Petch behavior

Let us start by considering that dislocations are line defects with length l. As we will see later, from an atomistic point of view, this length becomes increasingly important as the material's grain size reaches the nanoscale. Next, we shall assume that the nature of grain boundaries is not scale dependent. In fact, several investigations have revealed that the structure and width of grain boundaries is essentially the same for nanocrystalline materials and coarser-grained materials [47–49]. Finally, we shall consider that any grain boundary exhibits a specific probability to absorb a dislocation, on an atom by atom basis, as the dislocation approaches the grain boundary. However, instead of considering the particular crystallography of a grain boundary, the model proposed herein acknowledges the existence of distinct grain-boundary structures by assuming that each grain boundary exhibits a specific activation energy for dislocation absorption. This assumption will be discussed later in the paper in greater detail.

Assuming the probability of a dislocation being absorbed by the grain boundary to be P_{dis} and the probability of an individual atom on the dislocation core making the jump to be P_{atom}, a relatively simple analysis using a

Bernoulli distribution function can made. The Bernoulli function is a discrete distribution having two possible outcomes, labeled by $n = 0$ and $n = 1$, in which $n = 1$ (“success”) occurs with probability p and $n = 0$ (“failure”) occurs with probability $(1 - p)$, where $0 < p < 1$. Thus, p is the probability of an atom successfully jumping into the grain boundary in a single attempt, whereas $(1 - p)$ is the probability of an atom failing to make the jump in a single attempt. With this, we can write for P_{dis}, the following equation:

$$P_{\text{dis}} = P_{\text{atom}}^{J} = [1 - (1 - p)^{N}]^{J} \tag{2}$$

where J is the total number of atoms on the dislocation core jumping into the grain boundary. A value for J can be determined by multiplying the atomic linear density ζ of the dislocation core by the length l of the dislocation line. As the length of the dislocation line is proportional to the grain size d, the variable J is thus related to the grain size. N is the number of attempted jumps by dislocation core atoms to the grain boundary during an average time $\bar{t}$ between absorption of dislocations. N is defined by the product of the Debye frequency v, the time $\bar{t}$ and the Schmid factor C_{φ}. Thus, the $(1 - p)^{N}$ term in Eq. (2) represents the chance for one atom failing to make the jump after N attempts and the term $[1 - (1 - p)^{N}]$ describes the chance of one or more jump attempts succeeding. The probability p is thus a modified Boltzmann factor that represents the chance of an atom’s single jump attempt succeeding, when assisted by a shear stress τ. Hence, p is given by

$$p = \exp\left[-\left(\Delta G + \tau b^{3}\right)/k_{\text{B}}T\right] = \exp(M) \tag{3}$$

where ΔG is the activation energy for atomic migration, b is the Burgers vector, k_{B} is Boltzmann’s constant and T is temperature. M is thus a mobility factor. As we are describing the jump of atoms from the dislocation core to the grain boundary, ΔG is strongly dependent on the specific structure of the grain boundary, thereby implicitly taking into account the crystallographic nature of the grain boundary. Therefore Eq. (2) can be rewritten as

$$P_{\text{dis}} = \{1 - [1 - e^{M}]^{N}\}^{J} \tag{4}$$

From Eq. (4), immediate physical insight is possible. Because the term in the curly brackets is always less than 1, higher values of J will lower the probability P_{dis} of a dislocation being absorbed by the grain boundary. Hence, the larger the grain size d, the larger the value of J will be, and the lower will be the probability P_{dis}. On the other hand, as N is increased, the probability of all jump attempts failing decreases and thus the probability P_{dis} is increased. The reason for this behavior is due to the fact that N is the number of attempted jumps by dislocation core atoms to the grain boundary during an average time $\bar{t}$ between absorption of dislocations. Hence, as the time $\bar{t}$ is increased, N increases and thus the probability P_{dis} of dislocation absorption increases. In other words, this is a question of whether the absorption of dislocations by grain boundaries is fast enough to be relevant at reasonable strain rates. Assuming that the strain in the material is accommodated by the motion of dislocations, it is possible to determine the average time $\bar{t}$ during which an individual dislocation is able to traverse the entire grain. As the strain rate associated with the motion of one single dislocation is given by

$$\dot{\varepsilon} = \left(\frac{\bar{x}}{d}\frac{b}{d}\right)\Big/ t \tag{5}$$

where $\bar{x}$ is the average distance moved by the dislocation during the time t, then the average time $\bar{t}$ taken by each dislocation to cross the entire grain ($\bar{x} = d$) is given by $\bar{t} = b/(\dot{\varepsilon}d)$. Hence, the N factor can be rewritten as

$$N = (bC_{\phi}v)/\dot{\varepsilon}d \tag{6}$$

where the symbols have the same meaning as before. As a result, Eq. (4) shows that the probability of dislocation absorption by grain boundaries is strongly dependent on the grain size d and the strain rate $\dot{\varepsilon}$. As the absorption of dislocations by grain boundaries will obviously interfere with grain-boundary strengthening, Eq. (4) predicts that the greater the grain-boundary absorption that can occur, the more deviation from the Hall–Petch behavior (Eq. (1)) should be expected.

We are left with the task of establishing a correlation between the probability of dislocations being absorbed by grain boundaries and the classical Hall–Petch equation. To start, consider that the leading dislocation, in a pile-up of n dislocations, experiences a force due to (i) the resolved shear stress, τ, (ii) the other $(n - 1)$ dislocations and (iii) a backward force due to the internal stress τ_0 produced by the grain boundary. According to the classical Hall–Petch equation, the internal stress τ_0 is considered from the point of view of a rigid grain boundary, where dislocations pile up. This is the case where $P_{\text{dis}} = 0$ in Eq. (4). But, what happens when $P_{\text{dis}} \neq 0$? In this case, the grain boundary is no longer a rigid barrier and thus the internal stress τ_0 should be reduced to a term $\tau_0(1 - P_{\text{dis}})$. Assuming that the leading dislocation moves forward towards the grain boundary by a distance δx, the work done by the resolved shear stress can be described by $W_1 = nb\tau\delta x$. Therefore, the motion of the leading dislocation results in an increased interaction with the grain boundary, which can be described by $W_2 = b\tau_0(1 - P_{\text{dis}})\delta x$. At equilibrium, $W_1 = W_2$ and, hence, the resolved shear stress acting on the leading dislocation of a pile-up composed of n dislocations equals the backward force due to the internal stress τ_0 produced by the grain boundary. This can be expressed by

$$\tau_1 = \tau_0 = \frac{n\tau}{(1 - P_{\text{dis}})} \tag{7}$$

where the symbols have the same meaning as before. Assuming $n = d\tau/\mu b$ [35,36], where d is the grain size, τ is the resolved shear stress, μ is the shear modulus and b is the Burgers vector, Eq. (7) can be rewritten as

$$\tau^2 = \frac{\tau_1 \mu b (1 - P_{\text{dis}})}{d} \tag{8}$$

Considering the Schmid factor $C_\varphi = \cos\theta\cos\varphi$, then $\tau = \sigma\cos\theta\cos\varphi$ and $\tau_1 = \sigma_1\cos\theta\cos\varphi$, where σ is the applied stress, σ_1 is the critical stress at the leading dislocation to activate a dislocation source on an adjacent grain, θ is the angle between the tensile axis and the normal to the slip plane and φ is the angle between the tensile axis and the slip direction, Eq. (8) assumes the form

$$\sigma = \left[\frac{\sigma_1 \mu b}{\cos\theta\cos\varphi}\right]^{\frac{1}{2}}\left[\frac{1 - P_{\text{dis}}}{d}\right]^{\frac{1}{2}} \tag{9}$$

Assuming $k = \left[\frac{\sigma_1 \mu b}{\cos\theta\cos\varphi}\right]^{\frac{1}{2}}$, Eq. (9) becomes

$$\sigma = k\left[\frac{1 - P_{\text{dis}}}{d}\right]^{\frac{1}{2}} \tag{10}$$

which represents the yield strength of a material as a function of grain size and dislocation absorption by grain boundaries, when the lattice friction stress $\sigma_0 = 0$. In the presence of a lattice friction stress, the modified Hall–Petch relation can be expressed as

$$\sigma_y = \sigma_0 + k\left[\frac{1 - P_{\text{dis}}}{d}\right]^{\frac{1}{2}} \tag{11}$$

This equation describes the yield stress of a material as a function of grain size, taking into account the probability of grain-boundary absorption. Eq. (11) reverts to the classical Hall–Petch equation when the boundary is rigid and $P_{\text{dis}} = 0$. The essential effect of grain-boundary dislocation absorption is to reduce the number of dislocations, n, in the pile-up, which decreases the stress at the leading dislocation. If all moving dislocations are absorbed by the existing grain boundaries ($P_{\text{dis}} = 1$), then Eq. (11) is reduced to $\sigma_y = \sigma_0$, i.e., grain boundaries do not play any role in strengthening the material. In addition, as the term P_{dis} is negative in Eq. (11), reducing the Hall–Petch coefficient, k, is simply an inversion of the Hall–Petch relation.

3. Results and discussion

Eq. (11) can be evaluated for any material at a given temperature and strain rate. For illustration purposes, consider the case of Ni deformed at room temperature under a strain rate of $10^{-5}\,\text{s}^{-1}$. To determine P_{dis}, the resolved shear stress, τ, acting on the dislocations was assumed to be $\tau \approx \sigma_0 C_\varphi$ and $\sigma_0 = 21.8$ MPa [50]. For the Schmid factor C_φ, we assumed (i) a random orientation of grains with respect to the applied stress axis and (ii) a maximum stress direction on the slip plane. For an fcc material, the maximum angle possible between {1 1 1} slip planes is 109.48°, thus giving the average value

$$C_\phi \approx \int_{\theta=0}^{\theta=109/2} \cos(\theta)\sin(\theta) = 0.33$$

In addition, the following values were considered, namely $b = a/2[1\,1\,0] = 0.258$ nm, where $a = 0.365$ nm is the lattice parameter for Ni, $v = 10^{13}$ Hz and $\zeta = 6.54$ atoms/nm for the linear atomic density of the dislocation line in Ni. Finally, ΔG in Eq. (3) was assumed to be the activation energy for grain-boundary self-diffusion. This is a reasonable assumption as we are considering the absorption of atoms from the dislocation core into a grain boundary. For fcc metals, ΔG has been reported to vary within the range 0.6–1.5 eV [51] and thus a variety of activation energies were considered. One other reason to consider a variation in the activation energies is that grain boundaries with specific crystallographic structures will exhibit distinct abilities to absorb dislocations. Finally, assuming $k = 0.158$ MPa $\text{m}^{1/2}$ for the case of Ni [52], the yield stress σ_y in Eq. (11) can be plotted as a function of grain size for various activation energies (Fig. 1).

As shown in Fig. 1, for specific activation energies, there is a sharp transition at a critical grain size at which the yield stress is suddenly inverted. The critical yield stress (CYS) at which the transition occurs represents the onset of the inverse Hall–Petch behavior. At the highest activation energy examined (1 eV), the inverse Hall–Petch behavior would not be expected for Ni, even at unrealistically small grain sizes. On the other hand, for sufficiently small activation energies (0.75 eV), dislocation absorption in Ni would be expected to dominate.

Eq. (11) was also evaluated for different strain rates (Fig. 2a). Higher strain rates result in less deviation from the classical Hall–Petch relation, which results in higher CYS. Thus, higher strain rates and higher activation energies have a similar effect on the Hall–Petch behavior. Finally, calculations of Eq. (11) for different temperatures (Fig. 2b), predict that the CYS will be lower for higher temperatures and quite sensitive to temperature changes. Thus,

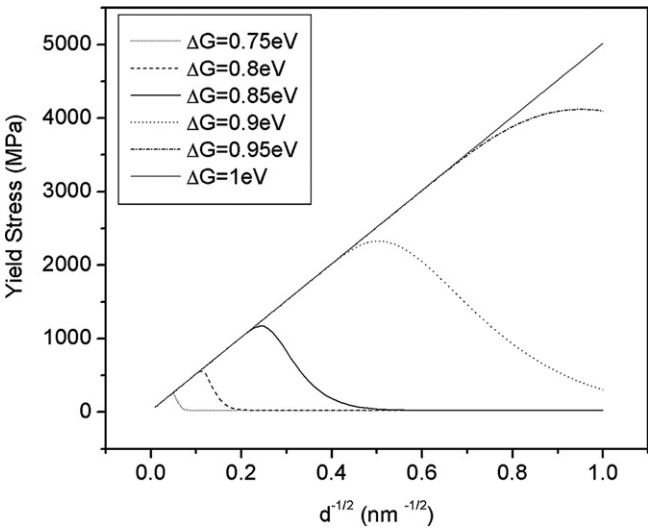

Fig. 1. The modified Hall–Petch relationship (Eq. (11)) for Ni deformed under a strain rate of $10^{-5}\,\text{s}^{-1}$ at 293 K, showing the inverse Hall–Petch effect at different critical grain sizes for various levels of activation energy.

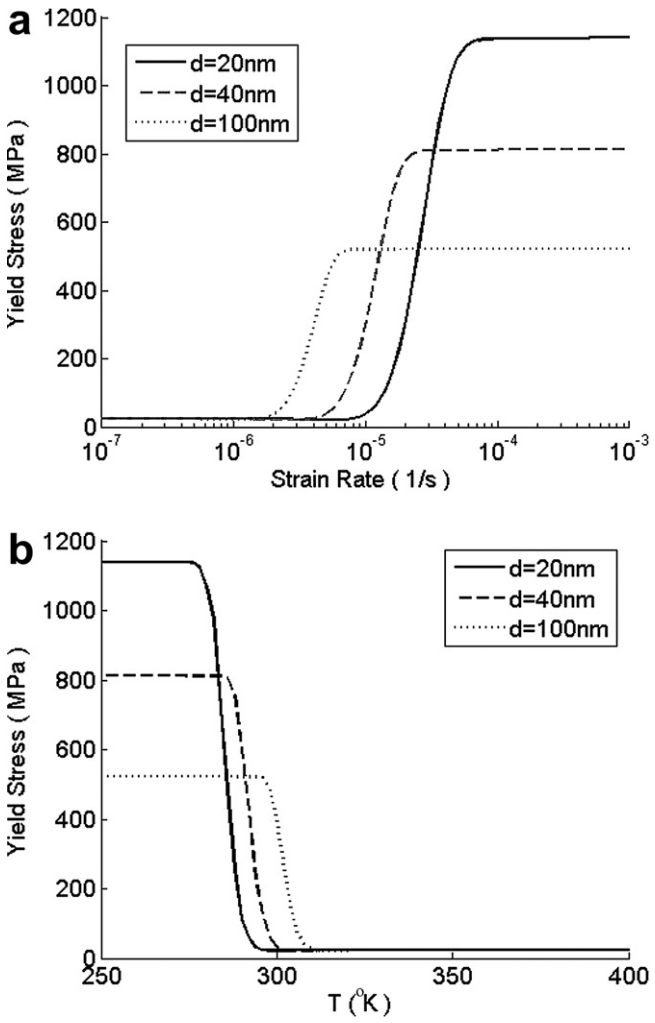

Fig. 2. (a) Yield stress vs. strain rate at a constant temperature of 293 K and (b) yield strength vs. temperature at a constant strain rate of 10^{-5}, in Ni for various grain sizes and an activation energy of 0.85 eV.

changes in temperature will have the opposite effect on the CYS to changes in activation energy and strain rate.

These predictions are theoretically and experimentally important for several reasons. First, the activation energy, which is typically proportional to the melting temperature, is expected to be different for distinct materials. In fact, calculations of Eq. (1) for Al, Cu and Ni reveal that a deviation from the Hall–Petch equation occurs earlier (coarser grain sizes) for Al, followed by Cu and Ni. Moreover, since the activation energy is correlated with grain-boundary structure, knowledge of the grain-boundary distribution becomes important to full understanding of the Hall–Petch behavior.

The model's second prediction is that the CYS depends significantly on strain rate, which confirms previous research [52–57]. This result is not surprising. As the strain rate is increased, more dislocations impinge on the grain boundaries per unit time. Therefore, less time is available for dislocations to be absorbed, leading to higher CYS at faster strain rates.

The third important prediction is that the CYS is very sensitive to temperature changes. As the temperature is increased, the probability for dislocation absorption increases, leading to stronger deviations from the Hall–Petch relation. Although work on the effect of temperature on the yield strength of nanocrystalline materials is sparse [52,58], the model suggests that experiments of this nature could help us understand the mechanisms of deformation in nanocrystalline materials.

In order properly to consider and confirm the results of the model, it is important to evaluate how the model fits the experimental data available in the literature. In doing so, a few issues arise. First, as tensile tests in nanocrystalline materials are difficult to perform, strain rates are frequently not recorded. This is problematic, as the strain rate is a very important parameter in the model described herein, while fitting the experimental data becomes very difficult if it is unknown. Second, the model assumes discrete values for the activation energy (grain-boundary self-diffusion) and for the grain size of the material. Yet, in real polycrystalline materials, a spread in activation energies (dictated by a distribution in grain-boundary structures) and a spread in available grain sizes is expected. Quantifying the effects of this spreading effect is not trivial and should be examined in future work. Third, the published data lack agreement due to the wide variety of experimental conditions employed, namely the use of different nanocrystalline materials, distinct methods of preparation (electrodeposited, severed deformed, powder compacted) and the use of either tensile tests under various strain rates and/or hardness tests.

An example of the variation in the Hall–Petch results for Ni using both tensile and hardness data is shown in Fig. 3. Although several studies claim evidence that either supports the classical [58–60] or the inverse Hall–Petch behavior [1,6,9,10], when the data for nanocrystalline Ni are viewed as a whole it becomes unclear whether it exhibits

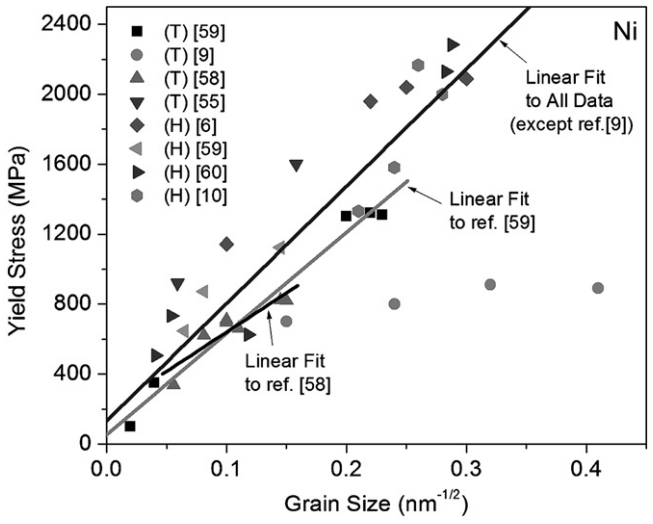

Fig. 3. Hall–Petch relationship for Ni determined by several research works. (T) denotes tensile tests and (H) denotes hardness tests.

an inverse Hall–Petch behavior. In fact, a linear regression performed on all the data, except for the data reported by Wang et al. [9], gives a correlation factor $R^2 = 0.93$. For some of the reported data [58,59] a linear regression fit gives correlation factors of $R^2 = 0.98$ and $R^2 = 0.84$, respectively.

According to our model, a lack of inverse Hall–Petch behavior in Ni would not be surprising. In fact, due to the high melting temperature of Ni and consequent high activation energy, we could expect it effectively to halt grain-boundary absorption of dislocations at reasonable strain rates. However, as mentioned above, polycrystalline materials exhibit a distribution of grain sizes and grain-boundary structures, which may lead to some form of deviation from the classical Hall–Petch relationship.

The model also suggests that the variation of results, such as those in Fig. 3, may differ due to differences in experimental conditions. If the strain rates used in the experiments differed significantly, or different methods for producing nanocrystalline materials lead to dissimilar grain-boundary distributions and grain size distributions, this in turn could result in distinct abilities for absorbing dislocations.

In the context of this discussion, it is valuable to consider the expected behavior of nanocrystalline copper, which has been widely investigated in the open literature [2,4,7,8,46,61–73], According to the model outlined above, copper would be more likely to exhibit an inverse Hall–Petch effect and/or exhibit a lower CYS than nickel. This is because the activation energy for dislocation absorption by grain boundaries for copper is lower than that of nickel. However, upon examination of the experimental results obtained for nanocrystalline copper (Fig. 4), the results reported are even more difficult to interpret than the results for nickel. As shown in Fig. 4, the two sets of data reported by Sanders et al. [8] appear to support the IHPE for a critical grain size of ~16 nm. On the other hand, the remainder of the data combined are highly inconclusive.

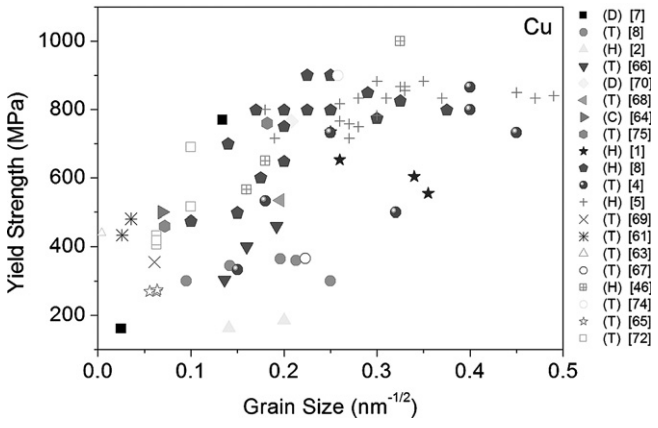

Fig. 4. Hall–Petch relationship for Cu determined by several research works. (D) denotes disk bending tests, (T) denotes tensile tests, (H) denotes hardness tests and (C) denotes compressive tests. See above-mentioned references for further information.

There are several possible explanations for this. It is possible that the samples indicating an IHPE were flawed in some way, for instance incomplete densification or the presence of an additional amorphous phase. It is also possible that, due to differences in the microstructure, some of the materials exhibited IHPE behavior while others did not. The theory presented above can rationalize this anomaly if the samples can be shown as having grain boundaries with substantially different activation energies of absorption.

Overall, the data obtained from individual research groups and shown in Fig. 4 seem to support the IHPE. However, when the data from single research groups are combined and viewed as a whole, the result is still ambiguous.

In the future, to overcome this ambiguity, it will become important to report the strain rate and the temperature used in the experiments, as well as to characterize the grain size distribution and grain-boundary structure.

4. Conclusions

The model presented herein uses a simple argument to produce a simple equation that can be used to make some interesting and useful predictions about the effects of grain-boundary strengthening in nanocrystalline materials. Simply, the model assumes a probability for atoms on a dislocation core to be absorbed by the grain boundary. The larger the grain size, the larger must be the number of atoms absorbed by the grain boundary, if the dislocation is also to be absorbed. Thus, for larger grain sizes, the probability for dislocation absorption by the grain boundary is lowered. The predictions provided by the model can be tested in the laboratory, keeping in mind that the strain rate, the temperature, grain-boundary distribution and grain size distribution are all important parameters to be considered. The results of future experiments dealing with these effects will help confirm this model and lead to an increase in our understanding of the mechanical properties of nanomaterials.

Acknowledgements

The authors would like to thank Professors Desiderio Kovar and Lew Rabenberg, from the University of Texas at Austin, for valuable discussions.

References

[1] Chokski AH, Rosen A, Karch J, Gleiter H. On the validity of the Hall–Petch relationship in nanocrystalline materials'. Scr Metall 1989;23:1679.
[2] Nieman GW, Weertman JR, Siegel RW. Microhardness of nanocrystalline palladium and copper produced by inert-gas condensation. Scr Metall 1989;23:2013.
[3] Lu K, Wei WD, Wang JT. Microhardness and fracture properties of nanocrystalline Ni–P alloy. Scr Metall Mater 1990;24:2319.
[4] Nieman GW, Weertman JR, Siegel RW. Mechanical behavior of nanocrystalline Cu and Pd. J Mater Res 1991;6:1012.

[5] Fougere GE, Weertman JR, Siegel RW, Kim S. Grain-size dependent hardening and softening of nanocrystalline Cu and Pd. Scr Metall Mater 1992;26:1879.
[6] El-Sherik AM, Erb U, Palumbo G, Aust KT. Deviations from Hall–Petch behavior in as-prepared nanocrystalline nickel. Scr Mater 1992;27:1185.
[7] Gertsman VY, Hoffmann M, Gleiter H, Dirringer R. Grain size dependence of yield of copper. Acta Mater 1994;42:3539.
[8] Sanders PG, Eastman JA, Weertman JR. Elastic and tensile behavior of nanocrystalline copper and palladium. Acta Mater 1997;10:4019.
[9] Wang N, Wang Z, Aust KT, Erb U. Room temperature creep behavior of nanocrystalline nickel produced by an electrodeposition technique. Mater Sci Eng A 1997;237:150.
[10] Schuh CA, Nieh TG, Yamasaki T. Hall–Petch breakdown manifested in abrasive wear resistance of nanocrystalline nickel. Scr Mater 2002;46:735.
[11] Giga A, Kimoto Y, Takigawa Y, Higashi K. Demonstration of an inverse Hall–Petch relationship in electrodeposited nanocrystalline Ni–W alloys through tensile testing. Scr Mater 2006;55:143.
[12] Nieh TG, Wadsworth J. Hall–Petch relation in nanocrystalline Solids. Scr Metall Mater 1991;25:955.
[13] Scattergood RO, Koch CC. A modified-model for Hall–Petch behavior in nanocrystalline materials. Scr Metall Mater 1992;27:1195.
[14] Lian B Buadelet, Nazarov A. Model for the prediction of the mechanical behavior of nanocrystalline materials. Mater Sci Eng A 1993;172:23.
[15] Malygin GA. Breakdown of the Hall–Petch law in micro- and nanocrystalline metals. Phys Solid State 1995;37:1248.
[16] Yamakov V, Wolf D, Phillpot SR, Muckherjee AK. Dislocation processes in the deformation of nanocrystalline aluminium by molecular-dynamics simulation. Nat Mater 2002;1:1.
[17] Schiotz J, Jacobsen K. A maximum strength of nanocrystalline copper. Science 2003;301:1357.
[18] Masamura RA, Hazzledine PM, Liaw PK, Lavernia EJ. Yield stress of fine grained materials. Acta Metall 1998;13:4527.
[19] Conrad H, Narayan J. On the grain size softening in nanocrystalline materials. Scr Mater 2000;42:1025.
[20] Van Swygenhoven H, Spaczer M, Caro A. Microscopic description of plasticity in computer generated metallic nanophase samples: a comparison between Cu and Ni. Acta Mater 1999;47:3117.
[21] Takeuchi S. The mechanism of the inverse Hall–Petch relation in nanocrystals. Scr Mater 2001;44:1483.
[22] Yamakov V, Wolf D, Salazar M, Phillpot SR, Gleiter H. Deformation mechanism crossover and mechanical behavior in nanocrystalline materials. Philos Mag Lett 2003;83:385.
[23] Yamakov V, Wolf D, Phillpot SR, Mukherjee AK, Gleiter H. Deformation-mechanism map for nanocrystalline metals by molecular dynamics simulation. Nat Mater 2004;3:43.
[24] Lu K, Sui ML. An explanation of the Hall–Petch law in micro and nanocrystalline materials. Scr Mater 1993;28:1465.
[25] Wang Ning, Wang Zhirui, Aust T, Erb U. Effect of grain size on the mechanical properties of nanocrystalline materials. Acta Metall Mater 1995;43:519–23.
[26] Konstantinidis DA, Aifantis EC. On the anomalous hardness of nanocrystalline materials. Nanostruct Mater 1998;10:1111.
[27] Song HW, Guo SR, Hu ZQ. A coherent polycrystal model for the inverse Hall–Petch relation in nanocrystalline materials. Nanostruct Mater 1999;11:203.
[28] Fan GJ, Choo H, Liaw PK, Lavernia EJ. A model for the inverse Hall–Petch relation of nanocrystalline materials. Mater Sci Eng A 2005;409:248.
[29] Chattopadhyay PP, Pabi SK, Manna I. On the inverse Hall–Petch relationship in nanocrystalline materials. Z Metall 2000;91:1049.
[30] Koch CC, Narayan J. The inverse Hall–Petch effect – fact or artifact. Mater Res Soc Symp 2001;634:B5.1.1.
[31] Kumar KS, Van Swygenhoven H, Suresh S. Mechanical behavior of nanocrystalline metals and alloys. Acta Mater 2003;51:5743.
[32] Zhu YT, Langdon TG. Influence of grain size on deformation mechanisms: an extension to nanocrystalline materials. Mater Sci Eng A 2005;409:234.
[33] Wolf D, Yamakov V, Phillpot SR, Mukherjee AK, Gleiter H. Deformation of nanocrystalline materials by molecular dynamics simulation: relationship to experiments. Acta Mater 2005;53:1.
[34] Meyers MA, Mishra A, Benson DJ. Mechanical properties of nanocrystalline materials. Progr Mater Sci 2006;51:427.
[35] Hall EO. The deformation and aging of mild steel. Proc Phys Soc London B 1951;64:747.
[36] Petch NJ. The cleavage strength of polycrystals. J Iron Steel Inst 1953;25:174.
[37] Eckert J, Holzer JC, Krill CE, Johnson WL. Structural and thermodynamic properties of nanocrystalline FCC metals prepared by mechanical attrition. J Mater Res 1992;7:1751.
[38] Milligan WW, Hackne SA, Ke M, Aifantis EC. In situ studies of deformation and fracture in nanophase materials. Nanostruct Mater 1993;2:267–76.
[39] Youngdahl CJ, Weertman JR, Hugo RC, Kung HH. Deformation behaviour in nanocrystalline copper. Scr Mater 2001;44:475–1478.
[40] Kumar KS, Suresh S, Chisholm MF, Horton JA, Wang P. Deformation of electrodeposited nanocrystalline nickel. Acta Mater 2003;51:397–405.
[41] Hugo RC, Kung HH, Weertman JR, Mitra R, Knapp JA, Follstaedt DM. In-situ TEM tensile testing of DC magnetron sputtered and pulsed laser deposited Ni thin films. Acta Mater 2003;51:1937.
[42] Shan Zhiwei, Stach EA, Wiezorek JMK, Knapp JA, Follstaedt DM, Mao SX. Grain boundary mediated plasticity in nanocrystalline nickel. Science 2004;305:654–7.
[43] Haque MA, Saif MTA. In situ tensile testing of nanoscale freestanding thin films inside a transmission electron microscope. J Mater Res 2005;20:1769–77.
[44] Hattar K, Han J, Saif MTA, Robertson IM. In situ transmission electron microscopy observations of toughening mechanisms in ultrafine grained columnar aluminum thin films. J Mater Res 2005;20:1869–77.
[45] Ma E. Watching the nanograins roll. Science 2004;305:623.
[46] Chen J, Lu L, Lu K. Hardness and strain rate sensitivity of nanocrystalline Cu. Scr Mater 2006;54:1913.
[47] Siegel RW, Thomas GJ. Grain boundaries in nanophase materials. Ultramicroscopy 1992;46:376.
[48] Van Swygenhoven H, Farkas D, Caro A. Grain boundary structures in polycrystalline metals at the nanoscale. Phys Rev B 2000;62:831.
[49] Kumar KS, Suresh S, Chisholm MF, Horton JA, Wang P. Deformation of electrodeposited nanocrystalline nickel. Acta Mater 2003;51:387.
[50] Thompson AW. Yielding in nickel as a function of grain or cell size. Acta Mater 1975;23:1337.
[51] Mehrer H, editor. Diffusion in solid metals and alloys. Series: Landolt-Bornstien: Numerical data and functional relationships in science and technology, Group 3, Condensed matter, vol. 26. Berlin: Springer Verlag; 1990.
[52] Gray GT, Lowe TC, Cady CM, Valiev RZ, Aleksandrov IV. Influence of strain rate and temperature on the mechanical response of ultra-fined grained Cu, Ni and Al–4Cu–0.5Zr. Nanostruct Mater 1997;9:477.
[53] Lu L, Li S, Lu K. An abnormal strain rate effect on tensile behavior in nanocrystalline copper. Scr Mater 2001;45:1163.
[54] Dalla Torre F, Van Swygenhoven H, Victoria M. Nanocrystalline electrodeposited Ni: microstructure and tensile properties. Acta Mater 2002;50:3957.
[55] Schwaiger R, Moser B, Dao M, Chollacoop N, Suresh S. Some critical experiments on the strain-rate sensitivity of nanocrystalline nickel. Acta Mater 2003;51:5159.
[56] Wei Q, Cheng S, Ramesh KT, Ma E. Effect of nanocrystalline and ultrafine grain sizes on the strain rate sensitivity and activation volume: FCC versus BCC metals. Mater Sci Eng A 2004;318:71.

[57] May J, Hoppel HW, Goken M. Strain rate sensitivity of ultrafine-grained aluminum processed by severe plastic deformation. Scr Mater 2005;53:189.
[58] Ebrahimi F, Bourne GR, Kelly MS, Matthews TE. Mechanical properties of nanocrystalline nickel produced by electrodeposition. Nanostruct Mater 1999;11:343.
[59] Xiao C, Mirshams RA, Whang SH, Yin WM. Tensile behavior and fracture in nickel and carbon doped nanocrystalline nickel. Mater Sci Eng A 2001;301:35.
[60] Hughes GD, Smith SD, Pande CS, Johnson HR, Armstrong RW. Hall–Petch strengthening for the microhardness of twelve nanometer grain diameter electrodeposited nickel. Scr Metall 1986;20:93.
[61] Merz MD, Dahlgren SD. Tensile-strength and work-hardening of ultrafine-grained high-purity copper. J Appl Phys 1975;46:3235.
[62] Hansen N, Ralph B. The strain and grain-size dependence of the flow-stress of copper. Acta Metall 1982;30:411.
[63] Embury DJ, Lahaie JD. In: Natasi M et al., editors. Mechanical properties and deformation behavior of materials having ultrafine microstructure. Dordrecht: Kluwer; 1993.
[64] Valiev Z, Kozolv E, Ivanov YF, Lian J, Nazarov AA, Baudelet R. Deformation behavior of ultra-fine-grained copper. Acta Mater 1994;42:2467.
[65] Ebrahimi F, Zhai Q, Kong D. Deformation and fracture of electrodeposited copper. Scr Mater 1998;39:315.
[66] Suryanarayanan IR, Frey CA, Sastry SML, Waller BE, Buhro WE. Mater Sci Eng A 1999;264:210.
[67] Lu L, Sui ML, Lu K. Superplastic extensibility of nanocrystalline copper at room temperature. Science 2000;287:1463.
[68] Legros M, Elliot BR, Rittner MN, Weertman JR, Hemker KJ. Microsample tensile testing of nanocrystalline metals. Philos Mag A 2000;80:1017.
[69] Huang HB, Spaepen F. Tensile testing of free-standing Cu, Ag and Al thin films and Ag/Cu multilayers. Acta Mater 2000;48:3261.
[70] Yousseff KM, Scattergood R, Murty KL, Koch CC. Ultratough nanocrystalline copper with a narrow size distribution. Appl Phys Lett 2004;85:929.
[71] Hansen N. Hall–Petch relation and boundary strengthening. Scr Mater 2004;51:801.
[72] Haouaoui M, Karaman I, Maier HJ, Hartwig KT. Microstructure evolution and mechanical behavior of bulk copper obtained by consolidation of micro- and nanopowders using equal-channel angular extrusion. Metall Mater Trans A 2004;35:2935.
[73] Hansen N. Boundary strengthening in undeformed and deformed polycrystals. Mater Sci Eng A 2005;409:39.
[74] Lu L, Shen Y, Chen X, Qian L, Lu K. Ultrahigh strength and high electrical conductivity in copper. Science 2004;304:422.
[75] Wang YM, Wang K, Pan D, Lu K, Hemker KJ, Ma E. Microsample tensile testing of nanocrystalline copper. Scr Mater 2003;48:1581.